

Molecular Engineering of Fluorene-Based Photosensitizers for Dye-Sensitized Solar Cells

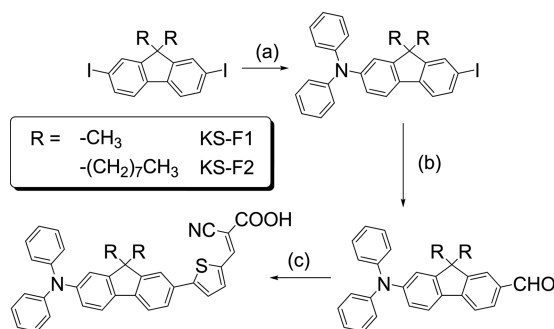
Se-Mi Kim, Mannix P. Balanay, Sang Hee Lee, and Dong Hee Kim*

Department of Chemistry, Kunsan National University, Gunsan 573-701, Korea. *E-mail: dhkim@kunsan.ac.kr
Received December 17, 2012, Accepted February 7, 2013

Key Words : Organic dye, Chenodeoxycholic acid, DSSC, Absorption spectra, Density functional theory

Fluorenes are very attractive as π -conjugated spacers in dye-sensitized solar cells (DSSCs) due to its higher molar extinction coefficients and more red-shifted spectra as compared to biphenyl moieties.¹ This is due to the co-planarity of two phenyl groups with the dialkyl group acting as a knot which could result in better π -conjugative properties, thus, larger charge-transfer transitions. The aggregation effect, which is caused by the increase planarity of the biphenyl group, can be controlled by introducing bulky alkyl groups at the 9,9-position of the fluorenyl moiety. A study of (9,9-diethyl-9*H*-fluorenyl)-based dye with increasing concentration of chenodeoxycholic acid (CDCA) as co-adsorbent showed that the short-circuit photocurrent density (J_{SC}) drastically decreased with increasing chenodeoxycholic acid concentration but the open-circuit voltage (V_{OC}) and fill factor (FF) slightly increased, which are commonly observed with dyes having CDCA co-sensitization. Overall, the solar-to-electric efficiency decreases with increasing CDCA concentration.² This indicates that the fluorenyl dye does not undergo serious aggregation effect. However, the bulkiness of the alkyl groups attached to the 9,9-position of the fluorenyl moiety should be properly assessed since it could influence the packing configuration, the coverage of the dye in the semiconductor surface, and the overall solar cell efficiency. In this communication, we assess the differences of the photovoltaic performances of the methyl or octyl as alkyl groups at the 9,9-position of the fluorenyl moiety.

The synthetic routes leading to the formation of the fluorene dyes are illustrated in Scheme 1 and the detailed procedure is



Scheme 1. (a) diphenylamine, 1,10-phenanthroline, CuCl, *t*-BuOK, toluene, 125 °C; (b) (5-formylthiophen-2-yl)boronic acid, cat. Pd(PPh₃)₄, Li₂CO₃, 3:1 dioxane/water mixture, 120 °C; (c) NCCH₂CO₂H, cat. piperidine, CH₃OH, reflux.

presented at the supporting information. The synthesis began with cross coupling of 2,7-diiodo-9,9-dialkyl-9*H*-fluorene with diphenylamine using a mixture of CuCl, *t*-BuOK, and 1,10-phenanthroline in dry toluene. The resulting intermediate were subjected to Suzuki coupling reaction with (5-formylthiophen-2-yl)boronic acid using Pd(PPh₃)₄ as catalyst and Li₂CO₃ in 3:1 dioxane/water. The aldehydes were converted to the desired dyes, KS-F1 and KS-F2, by Knoevenagel condensation reaction with cyanoacetic acid in the presence of piperidine.

The molecular structures of KS-F1 and KS-F2 optimized at mPWPW91/6-31G(d) with a 50% Hartree-Fock Exchange in gas phase using Gaussian 09 software³ are presented in Figure S1 (supporting information). This theoretical methodology was found to be very close with MP2 optimized geometries containing thiophene.⁴ The calculated molar volume of the analogues, were 380 and 582 cm³/mol for KS-F1 and KS-F2, respectively.

The absorption spectra of the analogues in THF solution and in film are shown in Figure 1. The introduction of the long alkyl chain does not have much effect on the shift of the absorption spectra in THF solvent, wherein KS-F2 has a λ_{max} of 422 nm compared to 421 nm of KS-F1. This is consistent with the similar charge-transfer properties of the dyes as depicted by the HOMO-LUMO spatial orientation (Figure S2, supporting information). However, the molar extinction coefficient of KS-F2 ($7.0 \times 10^3 \text{ M}^{-1} \text{ cm}^{-1}$) is 3 times lower than KS-F1 ($21.5 \times 10^3 \text{ M}^{-1} \text{ cm}^{-1}$). In the absorp-

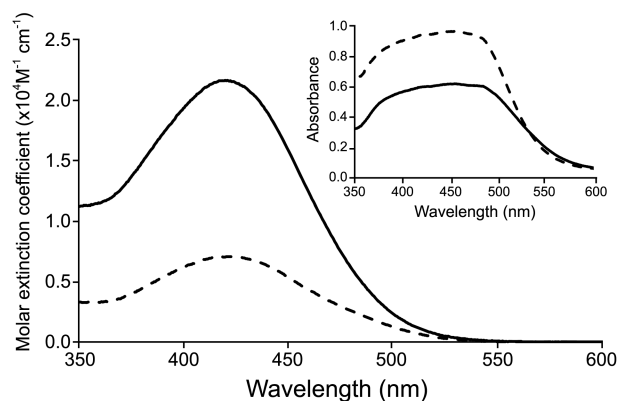


Figure 1. Absorption spectra of analogues KS-F1 (solid line) and KS-F2 (dashed line) in THF solution. The inset shows the absorption spectra of the analogues in TiO₂ film.

Table 1. Photovoltaic performances of the fluorenyl analogues^a

Dye	CDCA content (mM)	J_{sc} (mA cm ⁻²)	V_{oc} (mV)	FF (%)	η (%)	Amount of dye (nmol cm ⁻²)
KS-F1	0	10.27	652	66.7	4.47	78
	1	9.57	638	64.2	3.92	69
KS-F2	0	11.38	641	72.6	5.30	253
	1	11.42	645	71.8	5.29	183
N719		13.13	659	70.3	6.09	

^adata obtained using sealed cell under illumination of AM 1.5 with 0.159 cm² masking area using Oriel Sol3A solar simulator. The electrolyte consist of 0.6 M BMII, 0.04 M I₂, 0.025 M LiI, 0.05 M GuSCN, 0.28 M 4-*t*BP in 15:85 Val/MeCN. Fabrication of the cell was based on the doctor blade technique producing 10 + 5 mm TiO₂ film thickness. TiO₂ electrodes were immersed in 0.3 mM solutions for 32 H. For N719, 0.5 mM dye solutions for 20H, were used.

tion spectra of the dyes in film, both dyes exhibits similar λ_{max} at 455 nm but with KS-F2 having higher absorbance compared to KS-F1 which is a result of the higher amount of dye in film of KS-F2 than KS-F1 as shown in Table 1.

The higher photovoltaic performance (Table 1) of KS-F2 ($\eta = 5.30\%$) compared to KS-F1 ($\eta = 4.47\%$) is due to the higher amount of dye when absorbed in the TiO₂ surface producing a larger incident photon-to-current conversion efficiency (IPCE) or external quantum efficiency (EQE) with KS-F2 having an EQE of more than 80% ranging from 350 to 480 nm as shown in Figure 2. The IPCE data is consistent with the absorption spectra in film and their corresponding J_{sc} values shown in Figure 1 and Table 1, respectively. When compared with N719 using the same electrolyte, KS-F1 and KS-F2 achieved 73 and 87% of its solar cell efficiency.

The choice of the sensitizing solvent also has a crucial effect on the efficiency of the dye due to some reasons such as it could produce different amounts of dye, it has different dye-solvent interactions, and it results in various binding modes to the semiconductor surface.⁵ At this stage, THF was found to be the best solvent to give the highest photovoltaic performance as compared to pure or mixed solvents such as toluene, dimethylformamide, ethanol, acetonitrile, *tert*-butanol or combination thereof.

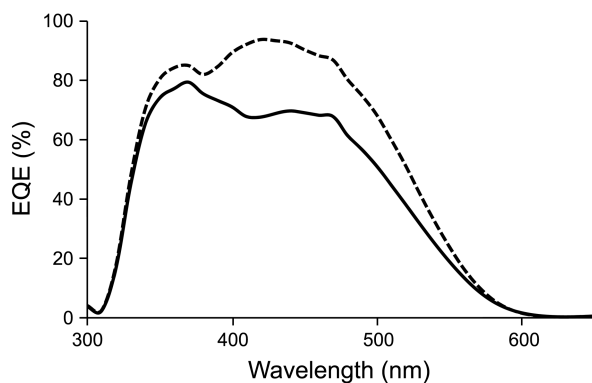


Figure 2. External quantum efficiencies (EQE) of analogues KS-F1 (solid line) and KS-F2 (dashed line) using Oriel QE-PV-SI QE/IPCE Measurement kit with silicon as reference cell.

The larger amount of dye in KS-F2 was due to its packing state in solution, wherein the long alkyl chains resulted in a loosely packed dye in solution making it adsorbed easily at the TiO₂ surface as also observed in infrared organic dyes.⁶ This is confirmed when we did an absorption analysis with increasing concentration of the dyes wherein it does not change the λ_{max} of KS-F2, whereas KS-F1 undergoes blue-shifting of its λ_{max} as the concentration increases (Figure S3, supporting information). The results suggest that KS-F2 exists as monomers in solution, while KS-F1 form H-type aggregates.

Another purpose of the long alkyl chain in KS-F2 is to minimize dye aggregation in film and at the same time block the redox-TiO₂ interactions. This was proven when 1 mM CDCA was added to the dyes, wherein KS-F2 with CDCA does not result in any significant changes in the photovoltaic performances, eventhough there is a decrease in the amount of dye. On the other hand, KS-F1 with CDCA produces lower efficiency.

In conclusion, these results demonstrate that the use of an octyl chain at the 9,9-position of the fluorenyl moiety can generate larger photocurrent by increasing the amount of dye at the semiconductor surface but with minimum dye aggregation. This information could help guide researchers in the proper design of an organic dye containing fluorenyl moieties. We are currently undertaking in our laboratory further assessment of more alkyl groups including branched alkyl chains to control effectively the packing of dyes at the TiO₂ surface. Furthermore, we are looking for more appropriate solvents to dissolve the dyes in order to attain highly efficient sensitizers for DSSCs.

Acknowledgments. This work was supported by the Basic Science Research Program through the National Research Foundation of Korea (NRF) funded by the Ministry of Education, Science and Technology (2010-0021818) and the KISTI supercomputing center through the strategic program for supercomputing application research (KSC-2012-C3-44).

References

1. (a) Hagfeldt, A.; Boschloo, G.; Sun, L.; Kloo, L.; Pettersson, H. *Chem. Rev.* **2010**, *110*, 6595. (b) Baheti, A.; Singh, P.; Justin Thomas, K. R. *Dyes Pigm.* **2011**, *88*, 195. (c) Baheti, A.; Tyagi, P.; Thomas, K. R. J.; Hsu, Y.-C.; Lin, J. T. s. *J. Phys. Chem. C* **2009**, *113*, 8541. (d) Chou, H.-H.; Hsu, C.-Y.; Hsu, Y.-C.; Lin, Y.-S.; Lin, J. T., *et al. Tetrahedron* **2012**, *68*, 767.
2. Lee, K.-M.; Suryanarayanan, V.; Ho, K.-C.; Justin Thomas, K. R.; Lin, J. T. *Sol. Energy Mater. Sol. Cells* **2007**, *91*, 1426.
3. Frisch, M. J.; Trucks, G. W.; Schlegel, H. B.; Scuseria, G. E.; Robb, M. A., *et al. Gaussian 09*, Revision B.01; Gaussian, Inc., Wallingford CT: 2010.
4. Balanay, M. P.; Kim, D. H. *J. Phys. Chem. C* **2011**, *115*, 19424.
5. (a) Balanay, M. P.; Kim, K. H.; Lee, S. H.; Kim, D. H. *J. Photochem. Photobiol. A* **2012**, *248*, 63. (b) Chang, D. W.; Tsao, H. N.; Salvatori, P.; De Angelis, F.; Gratzel, M., *et al. RSC Advances* **2012**, *2*, 6209. (c) Tian, H.; Yang, X.; Chen, R.; Zhang, R.; Hagfeldt, A., *et al. J. Phys. Chem. C* **2008**, *112*, 11023.
6. Ono, T.; Yamaguchi, T.; Arakawa, H. *J. Sol. Energy Eng.* **2010**, *132*, 021101.